

Recent developments and analyses in the **DEAP-3600** experiment

Akhil Maru

14th February, 2025



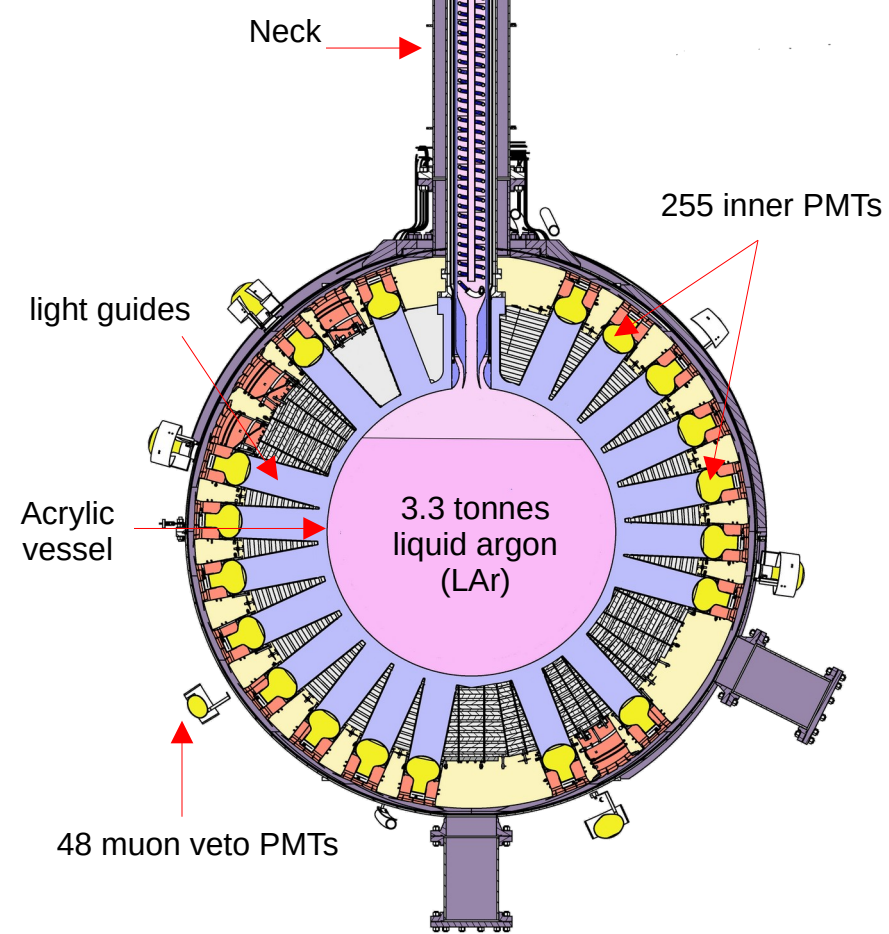
Outline

- DEAP-3600 experiment
- Results
 - ^{39}Ar specific activity measurement
 - ^{39}Ar half-life measurement
 - Quenching measurement
 - WIMP and Planck-scale DM search
- On-going analysis
 - Muon flux measurement
- Future!

Experiment

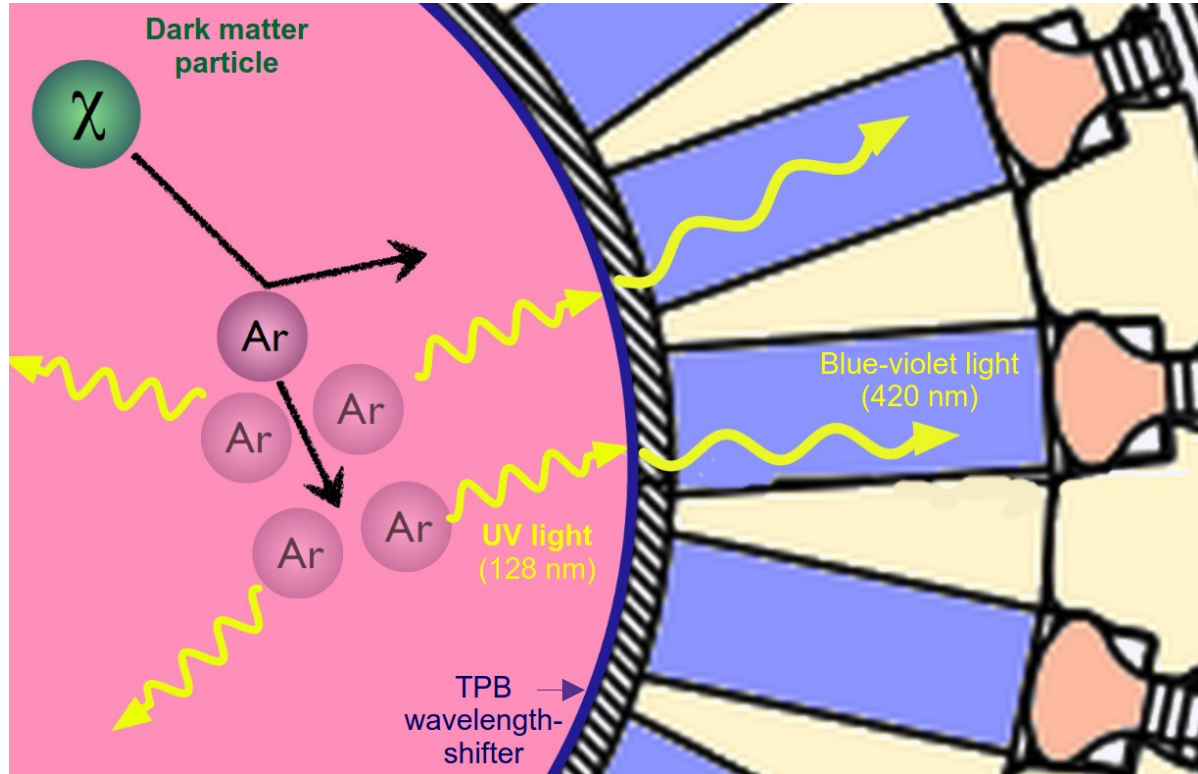
Detector

- Direct dark matter search experiment
 - **D**ark matter **E**xperiment using **A**rgon **P**ulse-shape discrimination (DEAP)
- (3269 ± 24) kg liquid argon (LAr)
- Located at SNOLAB, Sudbury
- ~ 2 km rock overburden (6000 m.w.e)



Water shielding

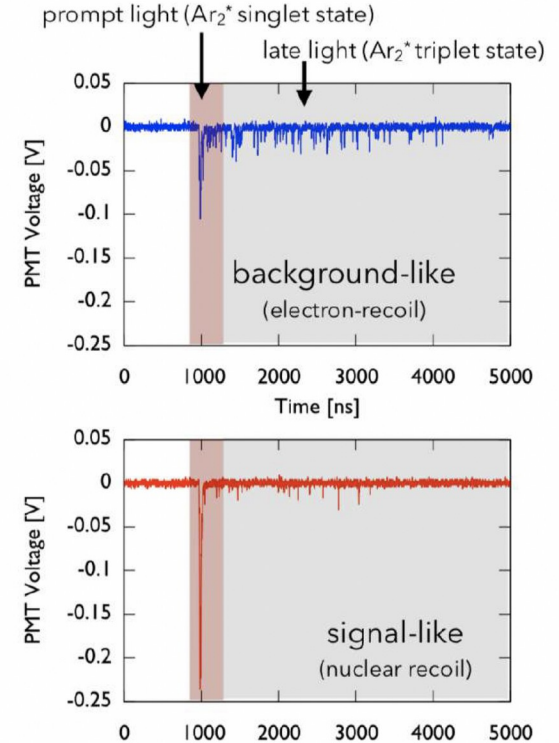
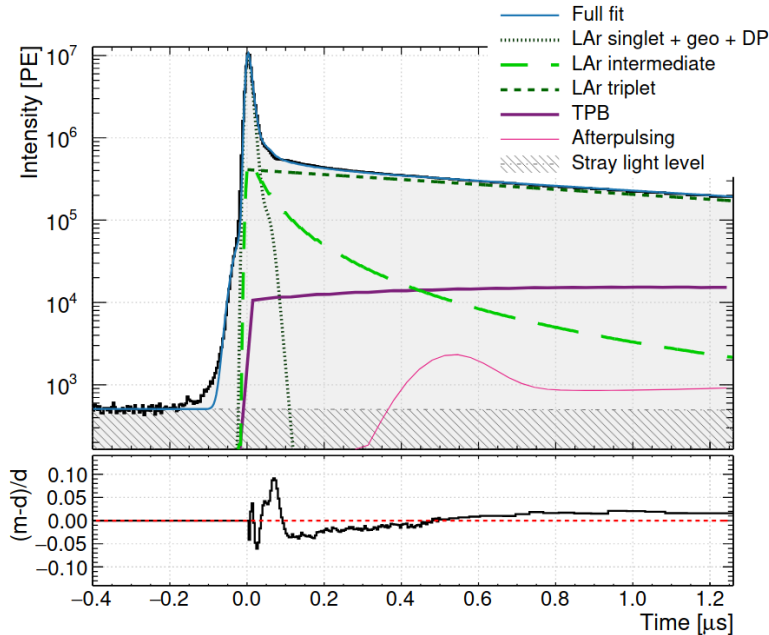
Detection



Pulse-shape discrimination (PSD)

- Pulse shape model:

$$PSD = \frac{\text{Prompt light}}{\text{Prompt light} + \text{Late light}}$$

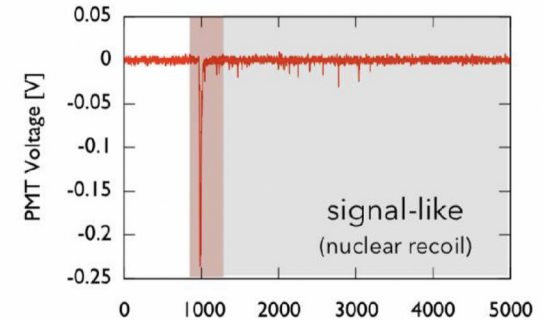
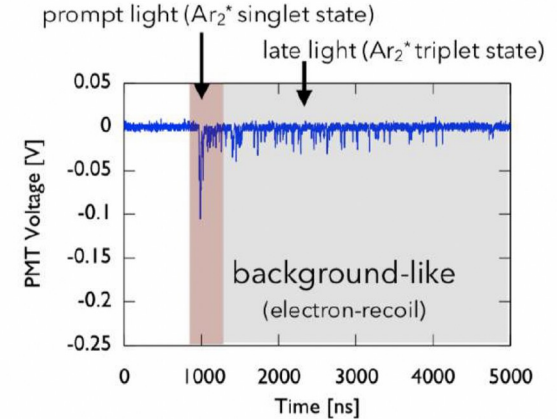
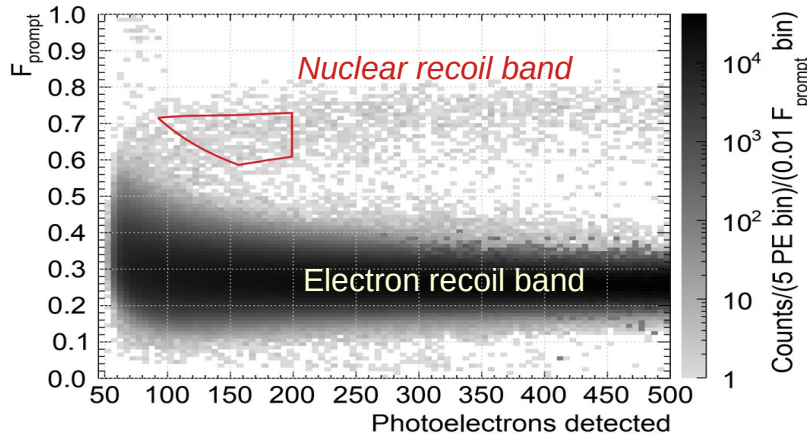


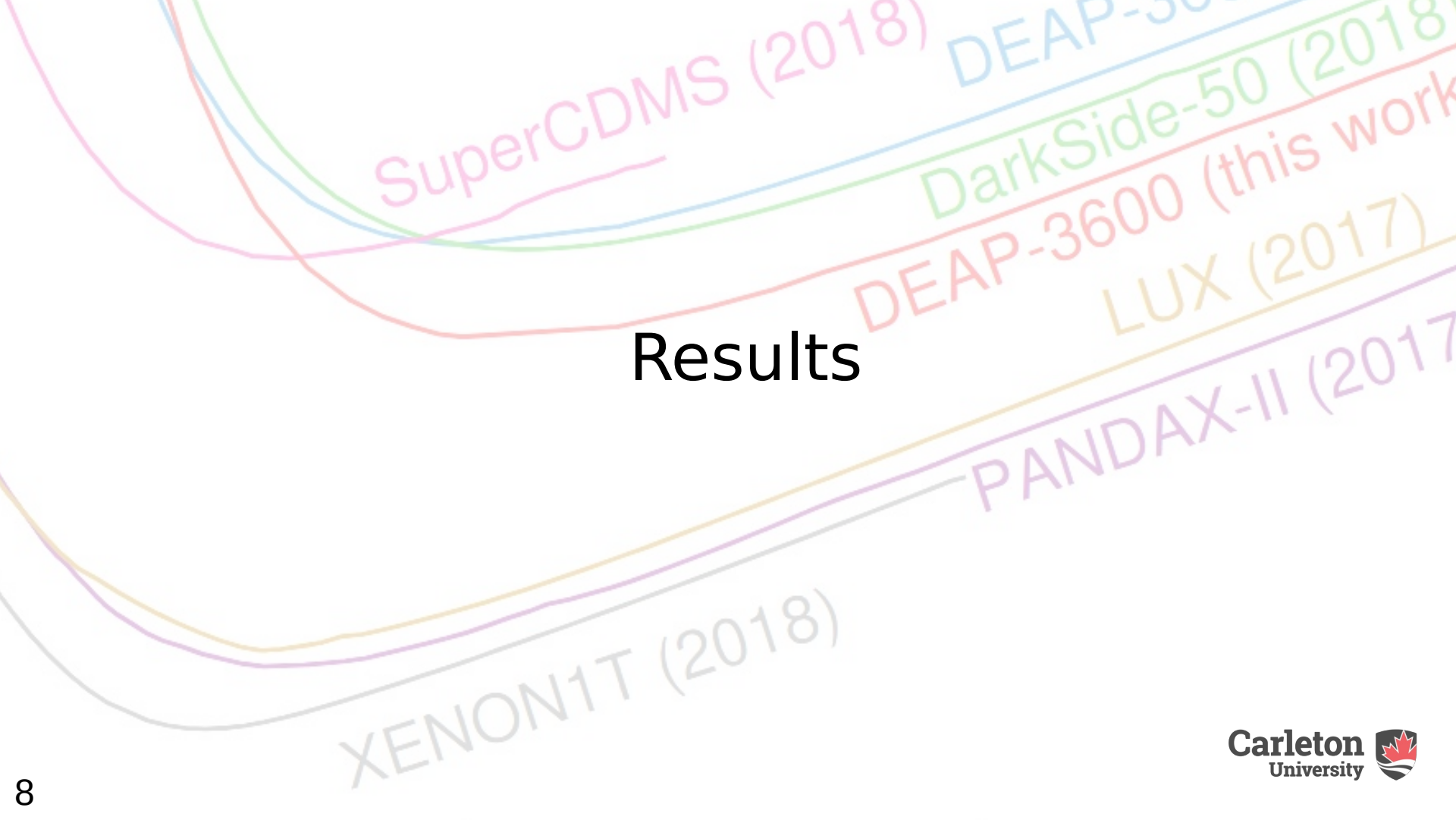
Pulse-shape discrimination (PSD)

- Pulse shape model:
- Nuclear recoil band and electron recoil band can be easily distinguished using this method
- Need to study the backgrounds thoroughly

$$PSD = \frac{\text{Prompt light}}{\text{Prompt light} + \text{Late light}}$$

$$F_{\text{prompt}} = \frac{\sum_{t=-28 \text{ ns}}^{t=150 \text{ ns}} Q(t)}{\sum_{t=-28 \text{ ns}}^{t=10 \text{ }\mu\text{s}} Q(t)}$$





SuperCDMS (2018)

DEAP-3600

DarkSide-50 (2018)

DEAP-3600 (this work)

LUX (2017)

PANDAX-II (2017)

XENON1T (2018)

Results

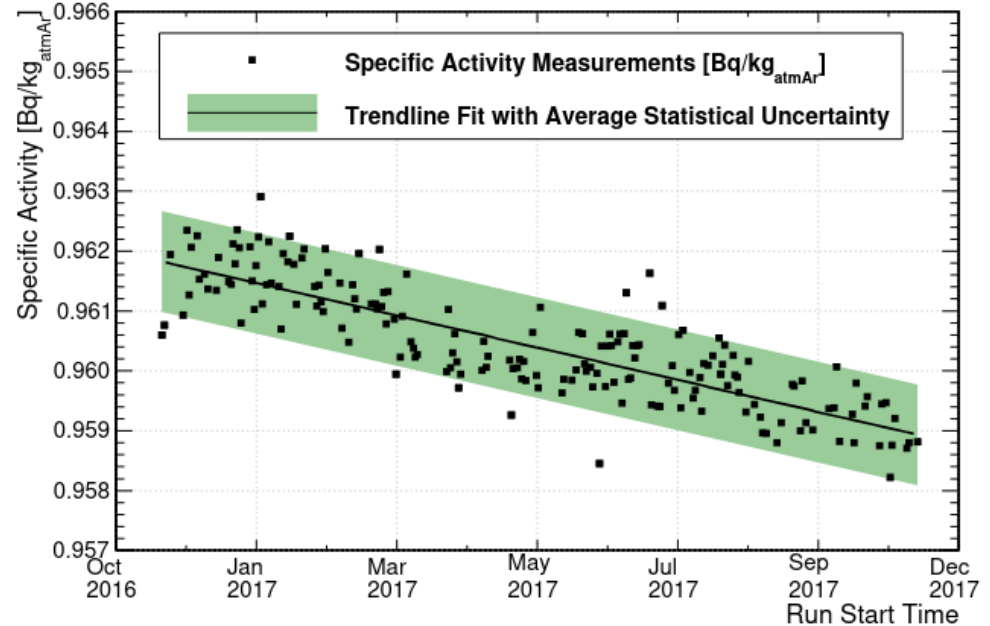
Results – ^{39}Ar specific activity measurement

- 167 live-days of data
- Specific activity

$$S_{\text{Ar}39} = \frac{N}{T_{\text{live}} \cdot m_{\text{LAR}}},$$

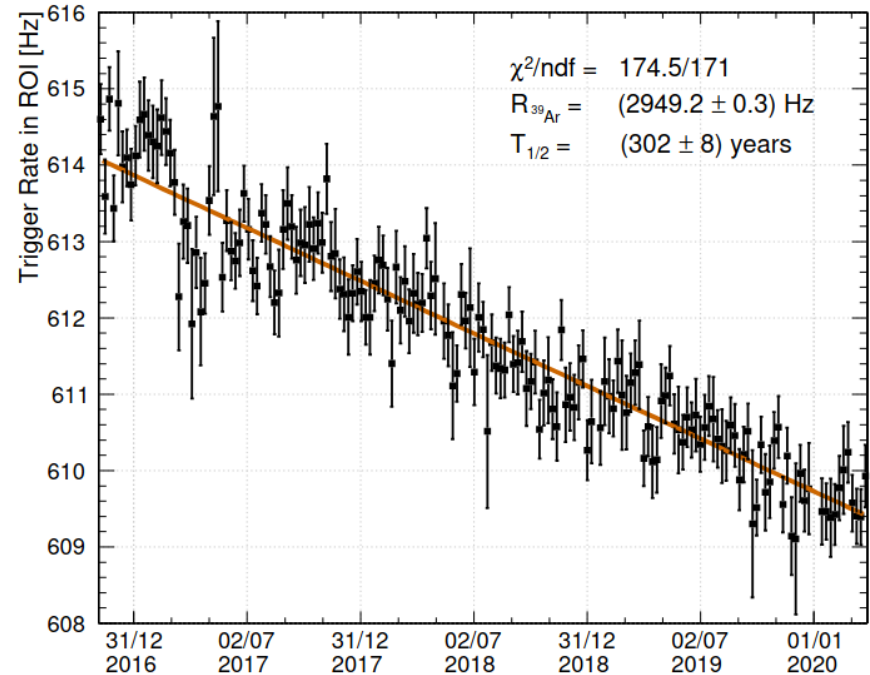
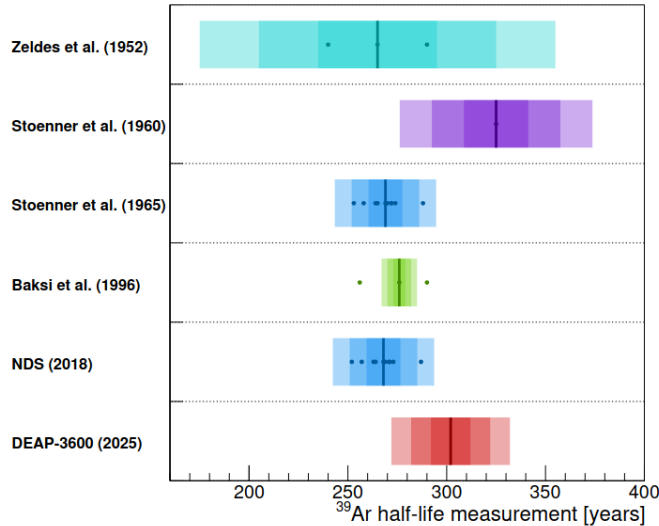
- Results:

| Measurement | Specific activity [Bq/kg _{atmAr}] |
|-----------------------|--|
| WARP [15] | $1.01 \pm 0.02_{\text{stat}} \pm 0.08_{\text{sys}}$ |
| ArDM [16] | 0.95 ± 0.05 |
| DEAP-3600 (this work) | $0.964 \pm 0.001_{\text{stat}} \pm 0.024_{\text{sys}}$ |



Results – ^{39}Ar half-life measurement

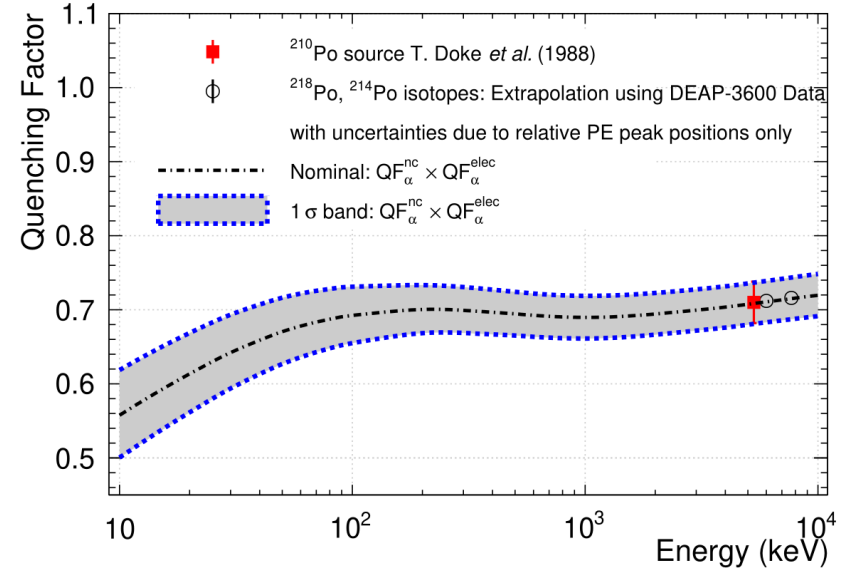
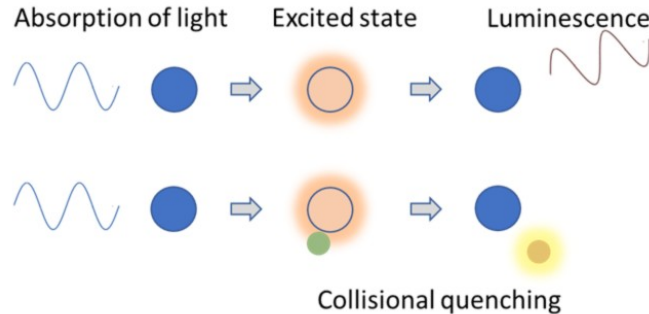
- First continuous direct measurement of ^{39}Ar decay
- 3.4 years of data



Results – Relative measurement and extrapolation of the quenching factor of α -particles in LAr

$$QF_{\alpha} = \frac{PE_{\alpha}}{Y \times E_{\alpha,dep}}$$

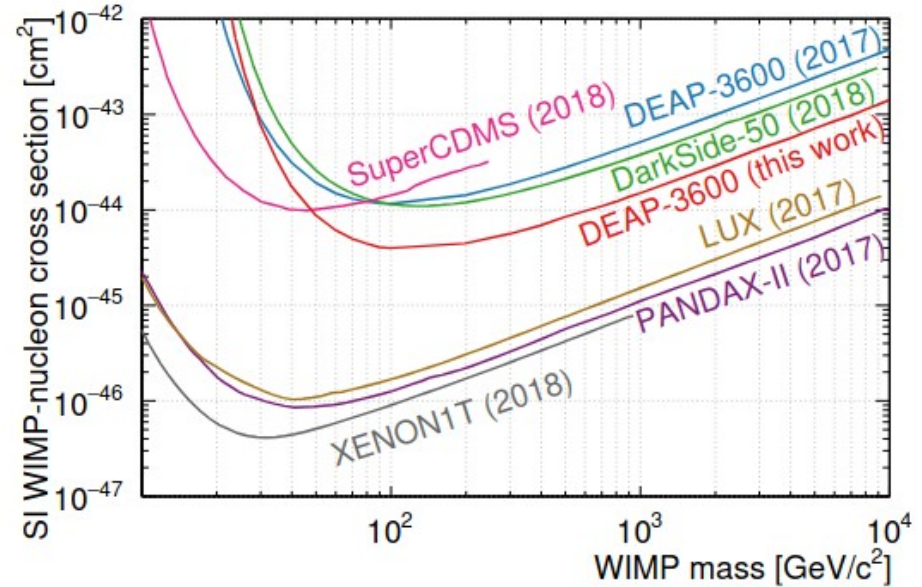
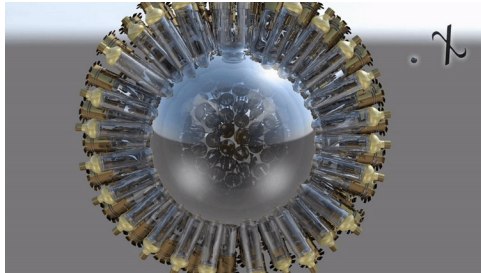
- Measure at full α -energy peaks
- Theoretical extrapolation to low energy



More about this in the next talk by Michael Perry

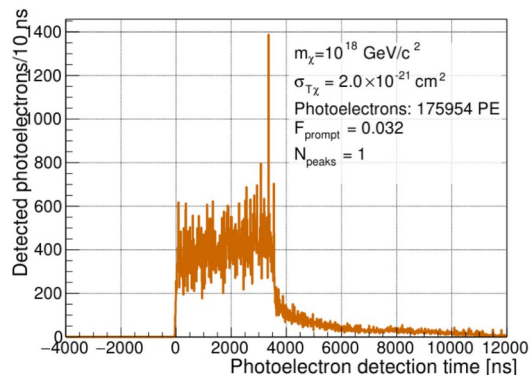
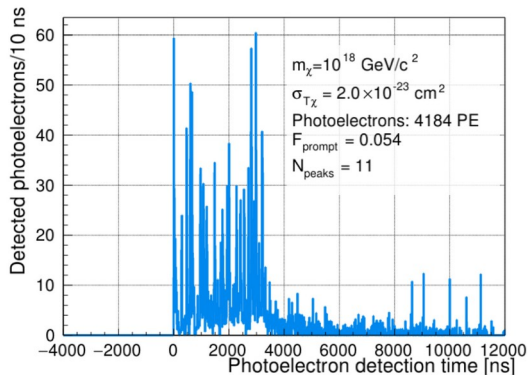
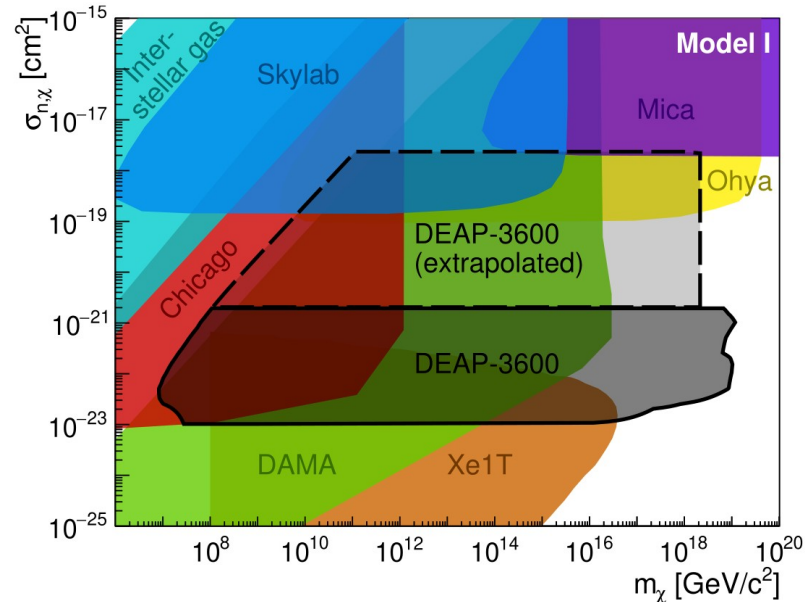
Results – WIMP dark matter search

- 231 live-days of data
- Leading limit on SI WIMP-nucleon cross section on LAr target
- No candidate signal events found
- Working on PLR analysis with the full dataset

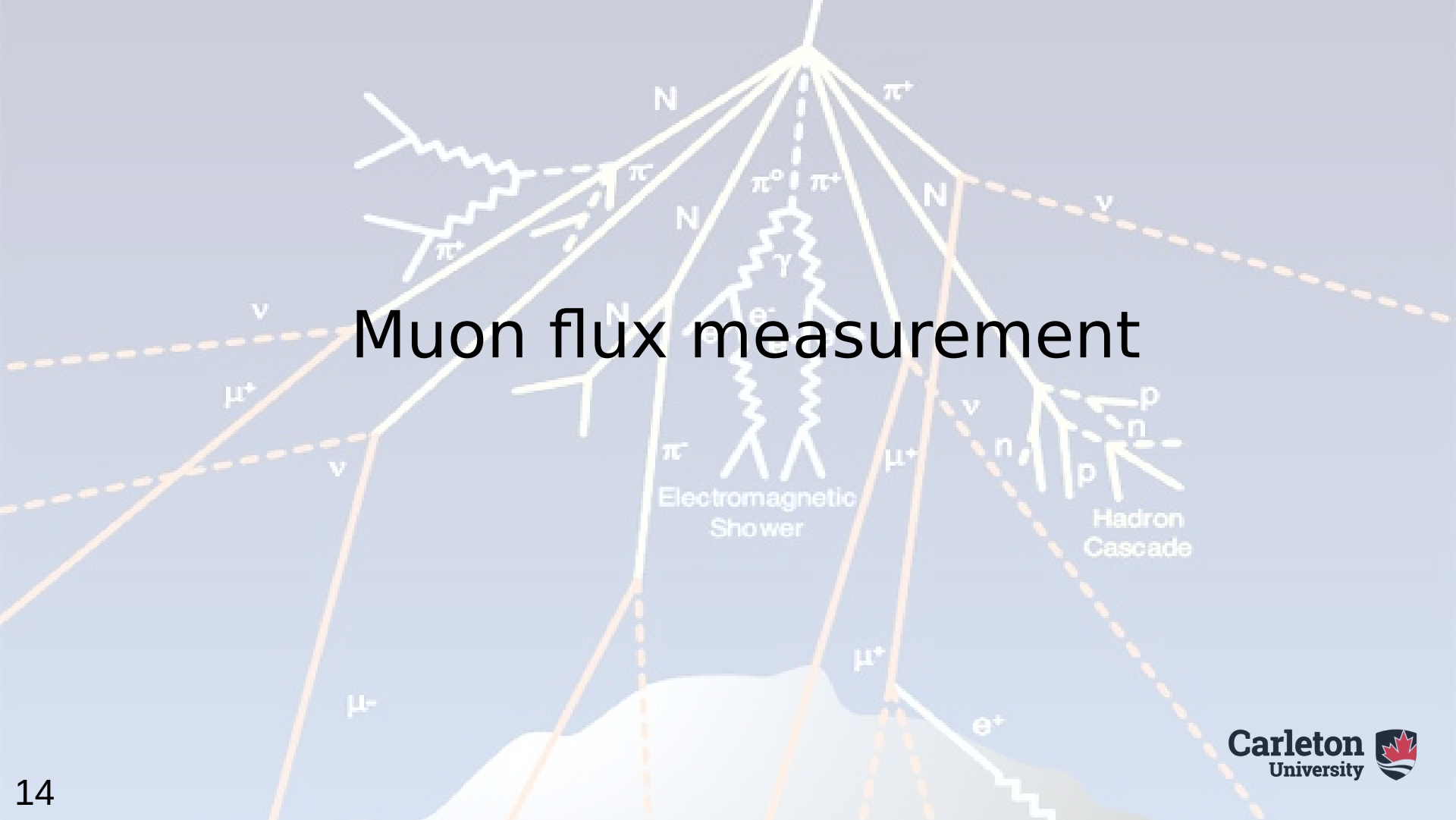


Results – Planck scale mass dark matter search

- First of its kind probe at Planck-scale mass ($m_\chi \simeq 10^{19} \text{ GeV}/c^2$) DM
- 813 live-days of data
- Look for very high energy events
- Multiple interaction in LAr



Muon flux measurement



Muon flux measurements!

- What do we need?

$$\textit{Muon Flux} = \frac{\textit{No. of Muons}}{\textit{Acceptance} \cdot \textit{Livetime} \cdot \textit{Effective Area}}$$

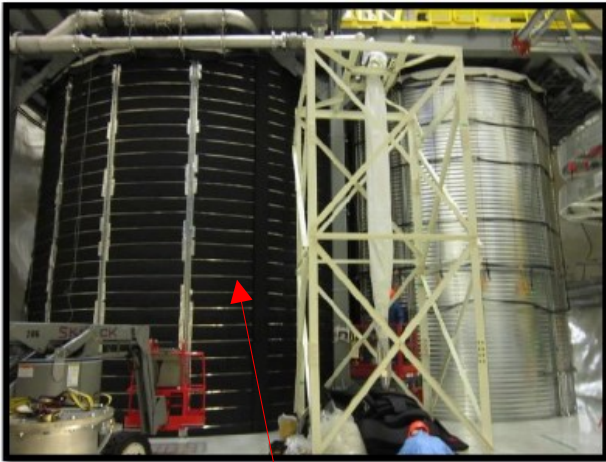
- Why do we need it?

Muons → cosmogenic neutrons → DM-like events → Bad!

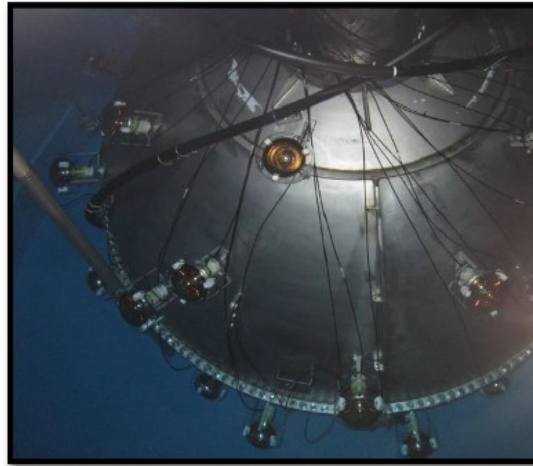
$$\text{Muon Flux} = \frac{\text{No. of Muons}}{\text{Acceptance} * \text{Livetime} * \text{Effective Area}}$$

Flux measurements!

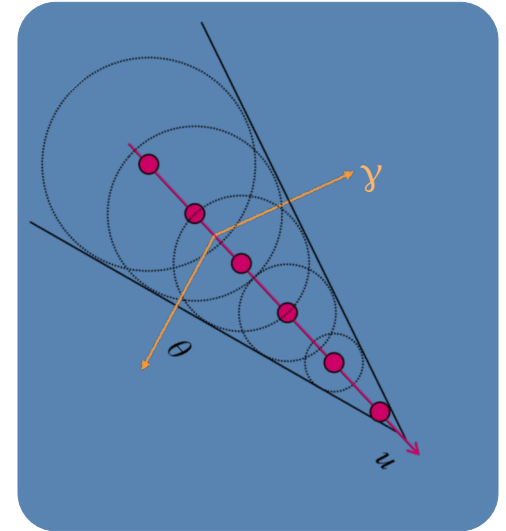
- Watertank data (MV)
 - #(muons) = 3395



DEAP-3600



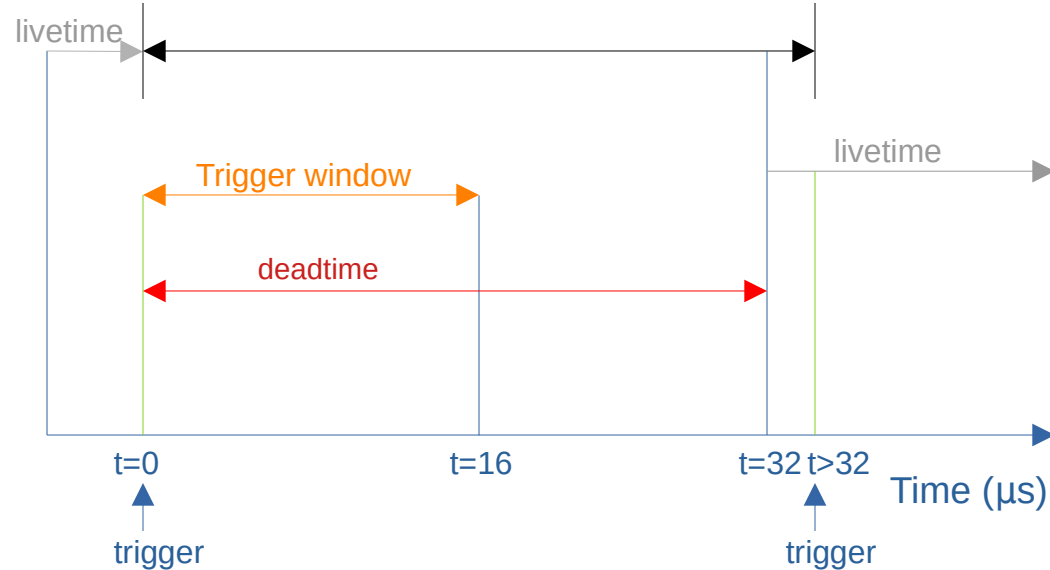
Cherenkov radiation in water



$$\text{Muon Flux} = \frac{\text{No. of Muons}}{\text{Acceptance} * \text{Livetime} * \text{Effective Area}}$$

Flux measurements!

- Livetime
 - Trigger counting
 - Runtime ~ 20-22 hr
 - Need to subtract deadtime between two events
 - Livetime = runtime – deadtime
 - $2.77 * 10^7$ s

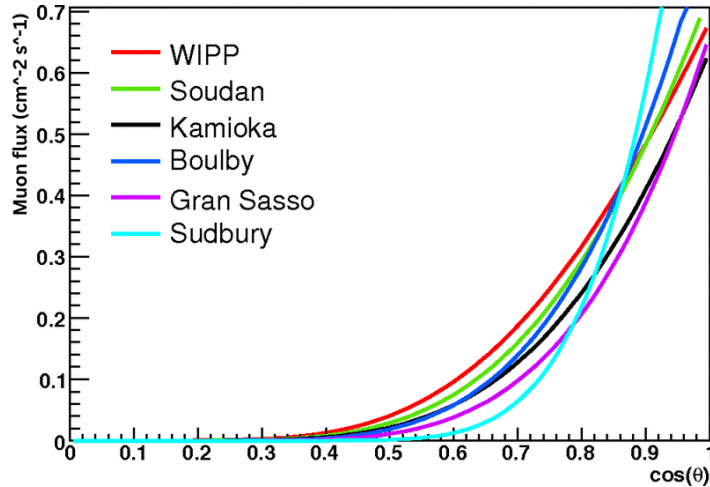


Flux measurements!

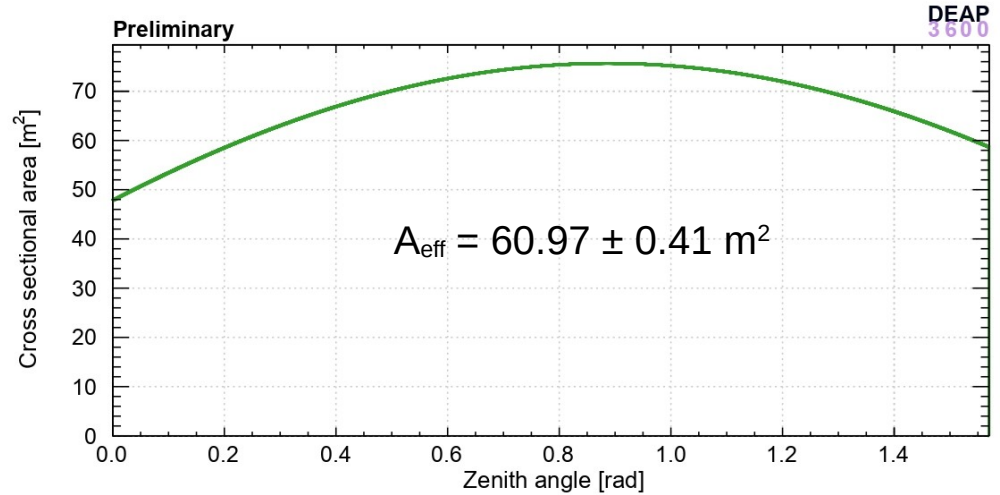
- Effective area

- $A_{\text{eff}} = 2\pi rh \sin\Theta + \pi r^2 \cos\Theta$

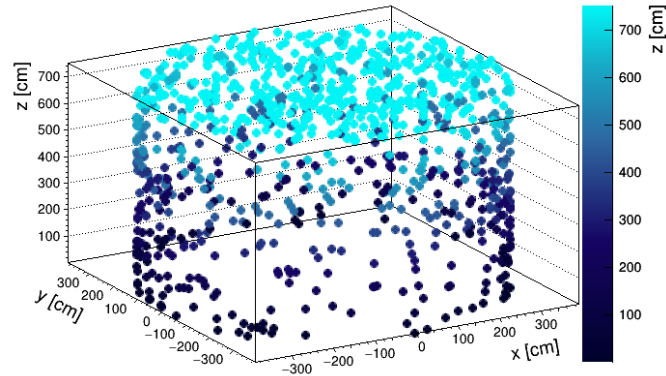
Mei-Hime angular distribution of muons



$$\text{Muon Flux} = \frac{\text{No. of Muons}}{\text{Acceptance} * \text{Livetime} * \text{Effective Area}}$$



Entry point of muons in DEAP watertank



Toy MC

$$\text{Muon Flux} = \frac{\text{No. of Muons}}{\text{Acceptance} * \text{Livetime} * \text{Effective Area}}$$

Flux measurements!

- Acceptances (*on-going*)
 - Matching simulation models to the data
 - External muGenCNL generator to simulate muons in RAT software
 - Tuning optical parameters of the detector in the simulation

$$\text{Acceptance} = \frac{\text{Number of events passing cuts}}{\text{Total number of events}}$$

```
//-----  
//  
// CNL Muon Generator  
//  
// Evan Rand, Canadian Nuclear Laboratories  
// evan.rand@cnl.ca  
//  
// Andrew Erlandson, CNL/Carleton  
// email Evan for questions or read the Mei & Hime paper  
//-----
```

- Optical Parameters:
 - QE: **Q**uantum **E**fficiency of the photocathode in the PMTs
 - TLR: **T**ank **L**iner **R**eflectivity of the watertank
 - ABSL: **A**bsorption **L**ength of the photons

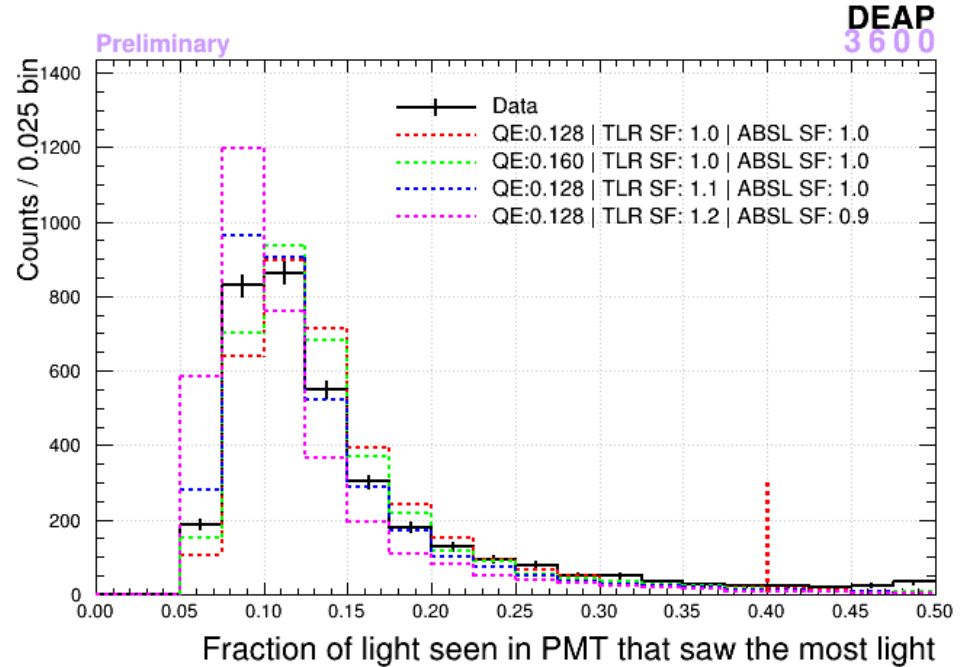
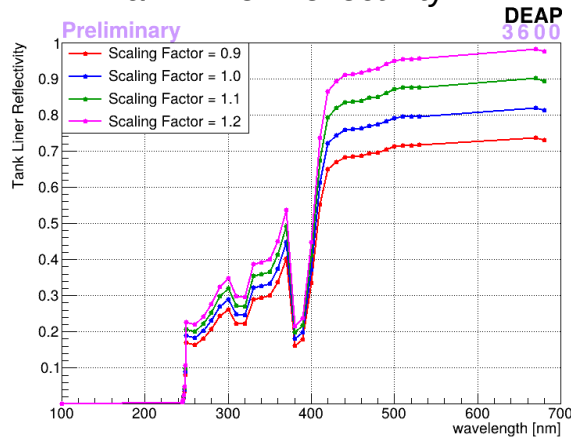
$$\text{Muon Flux} = \frac{\text{No. of Muons}}{\text{Acceptance} * \text{Livetime} * \text{Effective Area}}$$

Flux measurements!

- Watertank data (MV)
 - #(muons) = 3395
 - Livetime = $2.77 * 10^7$ s
 - Effective area = 60.97 ± 0.41 m²

- Acceptances (*on-going*)

- Tank Liner Reflectivity

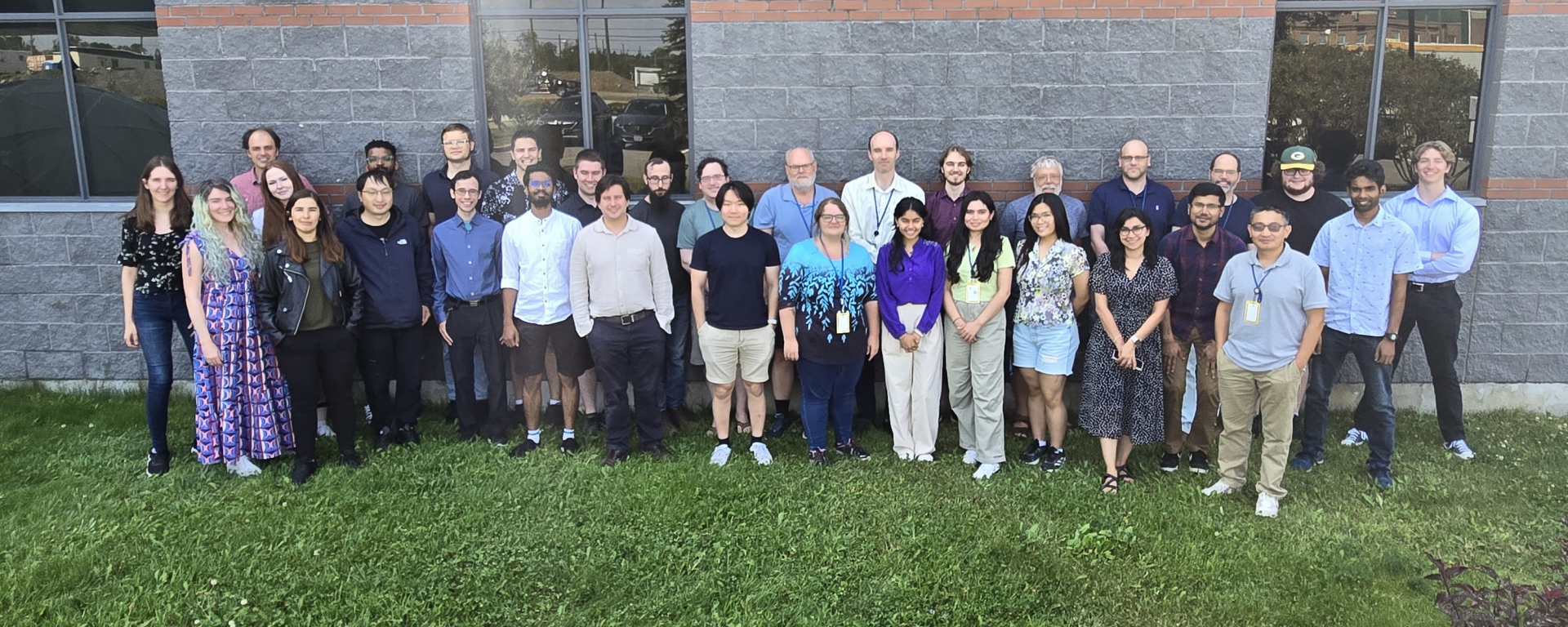




Future!

Future work

- Detector upgrades done!
- Third fill starts soon
- Multiple analyses close to done:
 - Muon flux measurement
 - WIMP search analysis
 - Neutrino absorption in LAr
- New results coming out soon! Stay tuned!



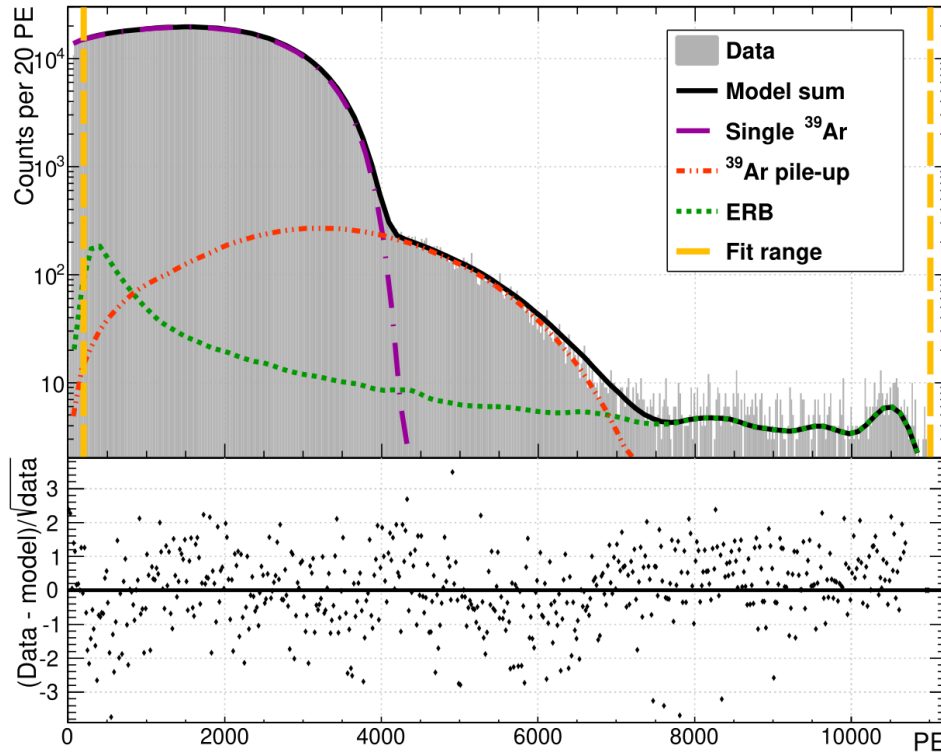
Thank You



Backup



Specific activity measurement of ^{39}Ar



$$N = N_{\text{single}} + N_{\text{pile-up}},$$

$$N_{\text{single}} = \frac{n \cdot a_{\text{presc}}}{\epsilon \cdot b},$$

$$N_{\text{pile-up}} = N_{\text{double}} + N_{\text{triple}} + N_{\text{ERB,Ar39}} + N_{\text{hFp,Ar39}}.$$

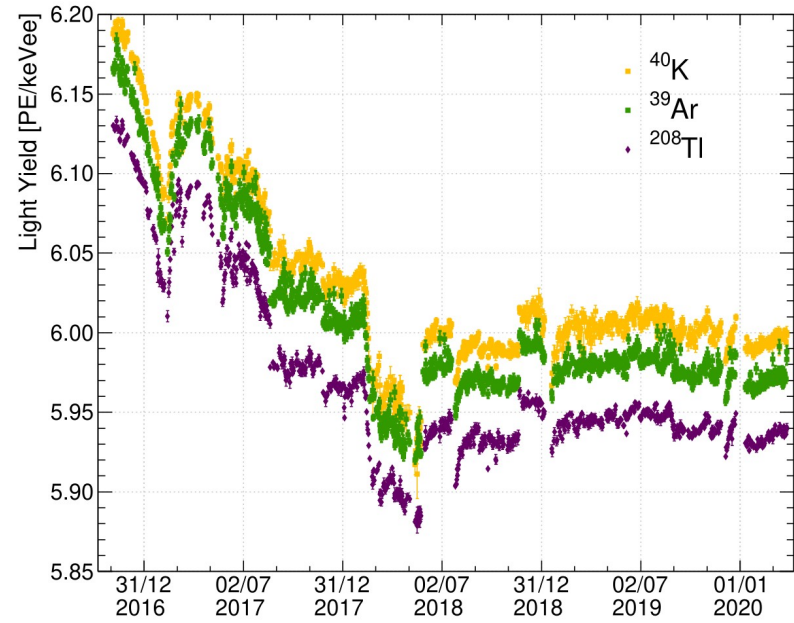
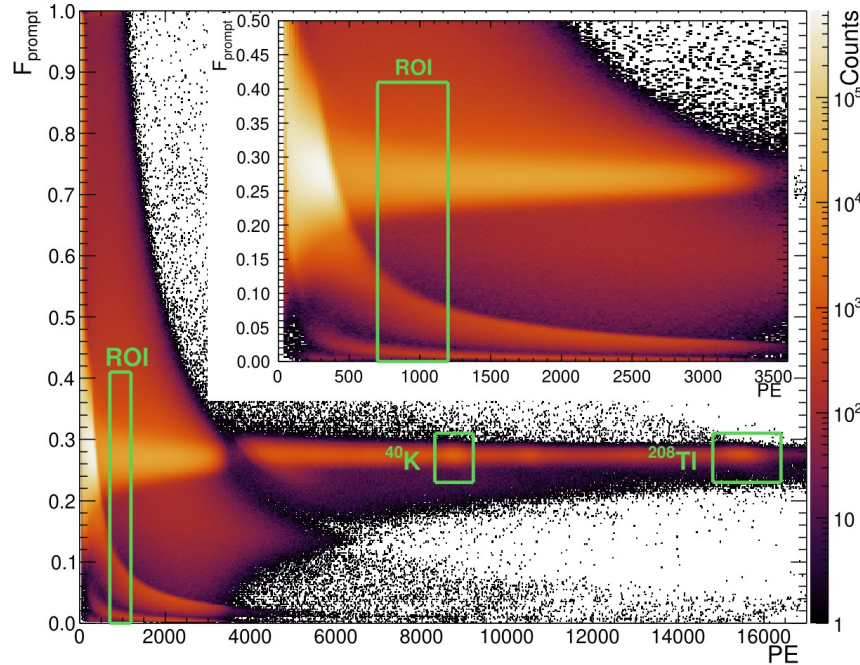
$$R_{\text{Ar39}} = \sqrt{\frac{N_{\text{double}}}{2 \cdot T_{\text{live}} \cdot \delta t_{\text{int}}}}.$$

Specific activity measurement of ^{39}Ar

Table 1 Parameters, their values and constraints, and the resulting contributions to the uncertainty for the specific activity measurement. Negligibly small systematic uncertainties are indicated with ‘–’. The dominant uncertainty on $S_{\text{Ar}39}$ arises from the uncertainties on event selection cut efficiency values as determined with the data-driven method (d-d) and the Monte Carlo method (MC).

| Parameter | Symbol | Value | Constraints | Absolute uncertainty on $S_{\text{Ar}39}$ [Bq/kg _{atmAr}] |
|--|----------------------------|-----------------------------|---|---|
| Fit range | | [200, 11000] PE | Fixed | 0.001 |
| Histogram bin width | b | 20 PE | Fixed | 0.001 |
| Constant energy scale parameter | p_0 | (1.3 ± 0.4) PE | Fixed | – |
| Linear energy scale term | p_1 | [7.1, 7.3] PE/keV | Free-floating, run-dependent | 0.009 |
| Quadratic energy scale term | p_2 | – | Not considered in this method | – |
| Linear resolution parameter | p_3 | [1.67, 1.73] PE | Free-floating, run-dependent | 0.009 |
| Quadratic resolution parameter | p_4 | $[2.1, 3.8] \times 10^{-4}$ | Free-floating, run-dependent | 0.001 |
| ^{39}Ar β -shape nuisance parameter | a_0 | | Free-floating, constrained by a penalty term | 0.001 |
| ^{39}Ar normalization | n | | Free floating, run-dependent | – |
| Double ^{39}Ar pile-up normalization | n_{double} | | Free floating, run-dependent | – |
| ERB normalization | n_{ERB} | | Free-floating, run-dependent | – |
| ^{85}Kr normalization | $n_{\text{Kr}85}$ | | Upper limit, see Section 5.2 | 0.010 |
| Liquid argon mass | m_{LAR} | (3269 ± 24) kg | Measured, see Section 3 | 0.007 |
| Live-time | T_{live} | 167 d [sum of all runs] | Measured, see Section 4 | – |
| Cut efficiency on single ^{39}Ar | ϵ | 0.983 [d-d], 0.999 [MC] | Measured, see Section 5.2 | 0.016 |
| Cut efficiency on double ^{39}Ar pile-up | ϵ_{double} | Run- & energy-dependent | | |

Half-life measurement of ^{39}Ar



$$\begin{aligned}
 R(t) = & e^{-R_{39\text{Ar}}(t)\delta t} \left[R_{39\text{Ar}}(t) f_1 \varepsilon_1 \right. \\
 & + \frac{1}{2} R_{39\text{Ar}}^2(t) \delta t f_2 \varepsilon_2 + \frac{1}{6} R_{39\text{Ar}}^3(t) \delta t^2 f_3 \varepsilon_3 \\
 & \left. + \frac{1}{2} R_{39\text{Ar}}(t) R_{\text{Chv}} e^{-R_{\text{Chv}}\delta t} \delta t f_4 \varepsilon_4 \right] + R_{\text{bg}}.
 \end{aligned}$$

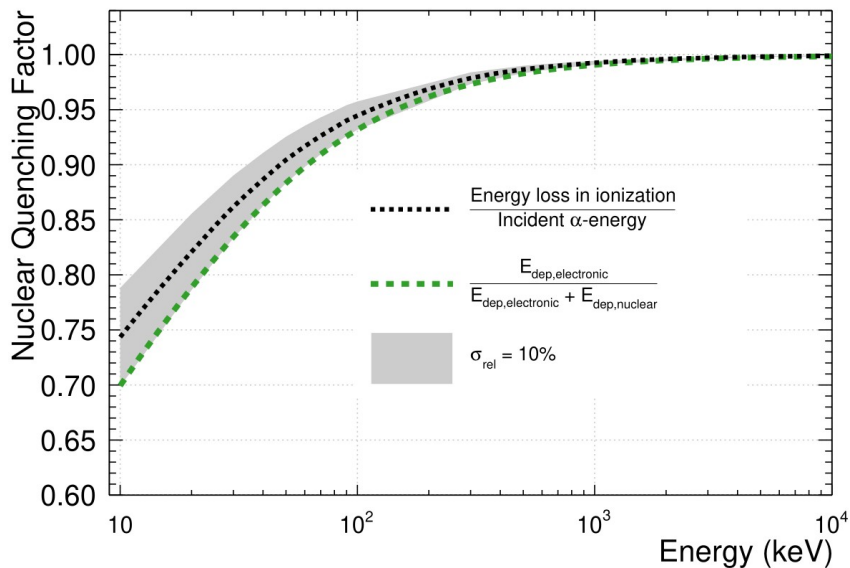
Half-life measurement of ^{39}Ar

Table 2 List of parameters used in the model of ^{39}Ar trigger rates (Sections 4, 5) along with their uncertainties. The uncertainties due to the event selection efficiencies for each event type are given as a combined value. The uncertainties are estimated with respect to the measured mean lifetime and converted to half-life values. The character ‘–’ indicates a negligibly small uncertainty.

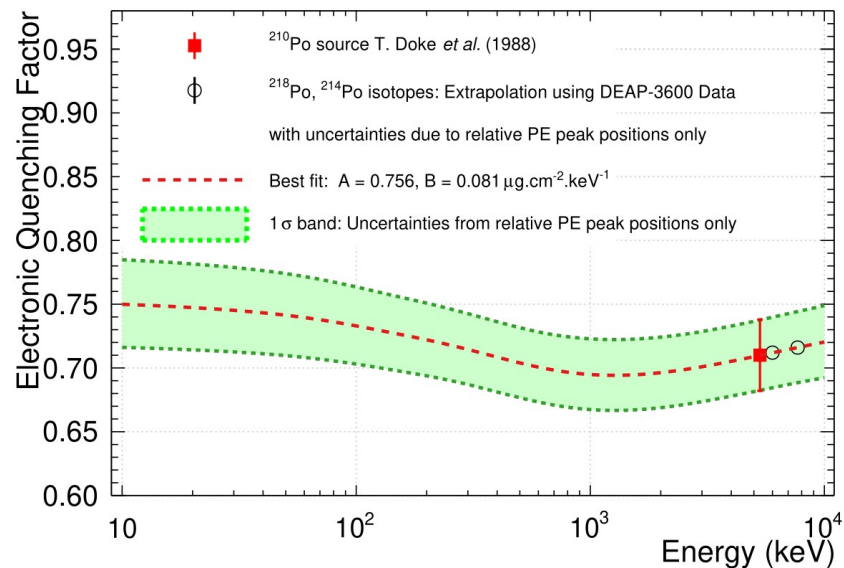
| Parameter | Symbol | Value | Constraints | Absolute uncertainty on $T_{1/2}$ [years] |
|---|-------------------------|----------------------|---------------|---|
| ^{39}Ar trigger rate at dataset start | $R_{^{39}\text{Ar}}$ | | Free-floating | |
| ^{39}Ar lifetime | $\tau_{^{39}\text{Ar}}$ | | Free-floating | |
| Cherenkov trigger rate | R_{Chv} | (538 ± 4) Hz | Fixed | – |
| ERB background rate | R_{bg} | (1.65 ± 0.31) Hz | Fixed | 0.15 |
| Livetime | T_{live} | 1.80 years | Fixed | – |
| Bin width for trigger rate averages | | 7 days | Fixed | 1.3 |
| Fraction of single ^{39}Ar spectrum in the ROI | f_1 | 0.21 ± 0.05 | Fixed | 0.21 |
| Cut efficiency for single ^{39}Ar | ϵ_1 | 1 | Fixed | – |
| Fraction of double ^{39}Ar spectrum in the ROI | f_2 | 0.20 ± 0.05 | Fixed | 1.1 |
| Cut efficiency for double ^{39}Ar | ϵ_2 | 0.9099 ± 0.0033 | Fixed | 1.8 |
| Fraction of triple ^{39}Ar spectrum in the ROI | f_3 | 0.19 ± 0.05 | Fixed | 0.01 |
| Cut efficiency for triple ^{39}Ar | ϵ_3 | 0.860 ± 0.039 | Fixed | 0.19 |
| Fraction of ^{39}Ar -Cherenkov pile-up spectrum in the ROI | f_4 | 0.21 ± 0.05 | Fixed | 0.04 |
| Cut efficiency for ^{39}Ar -Cherenkov pile-up | ϵ_4 | 1 | Fixed | – |
| Light yield corrections (constant) | | Run-dependent | N/A | 2.3 |
| Light yield corrections (differential) | | Run-dependent | N/A | 5.1 |
| Correlated triggers | | Run-dependent | N/A | 2.1 |

Quenching factor extrapolation

$$QF_{\alpha}^{\text{nucl}} = \frac{E_{\text{dep,elec}}}{E_{\text{dep,elec}} + E_{\text{dep,nucl}}}$$



$$QF_{\alpha}^M = \frac{y(E_{\alpha})}{E_{\alpha}} = \frac{A}{E_{\alpha}} \int_0^{E_{\alpha}} \frac{dE}{1 + B \frac{dE}{dx}}$$



Quenching factor extrapolation

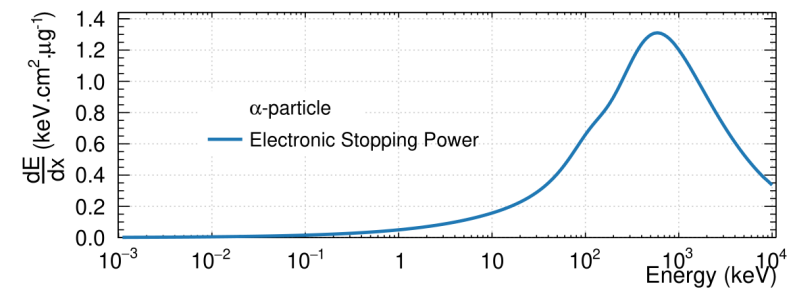
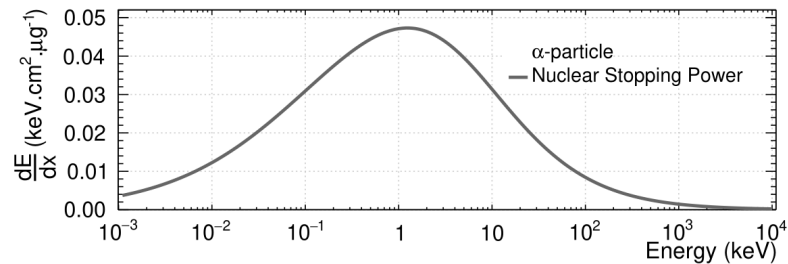
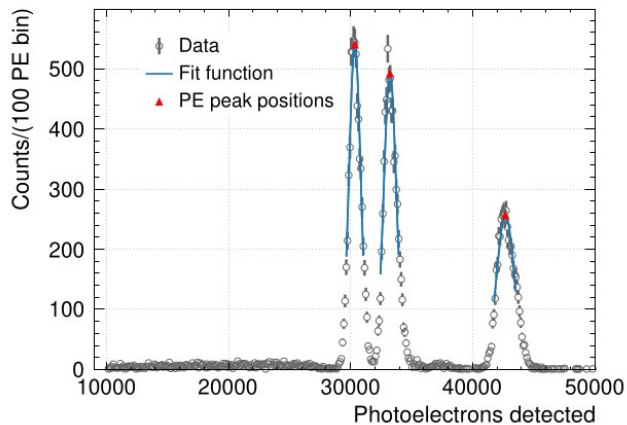
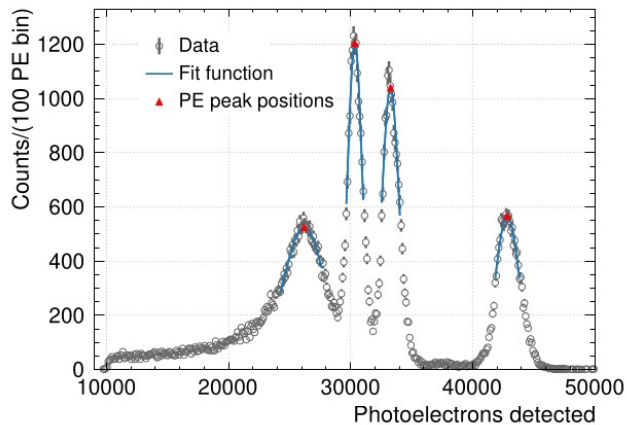
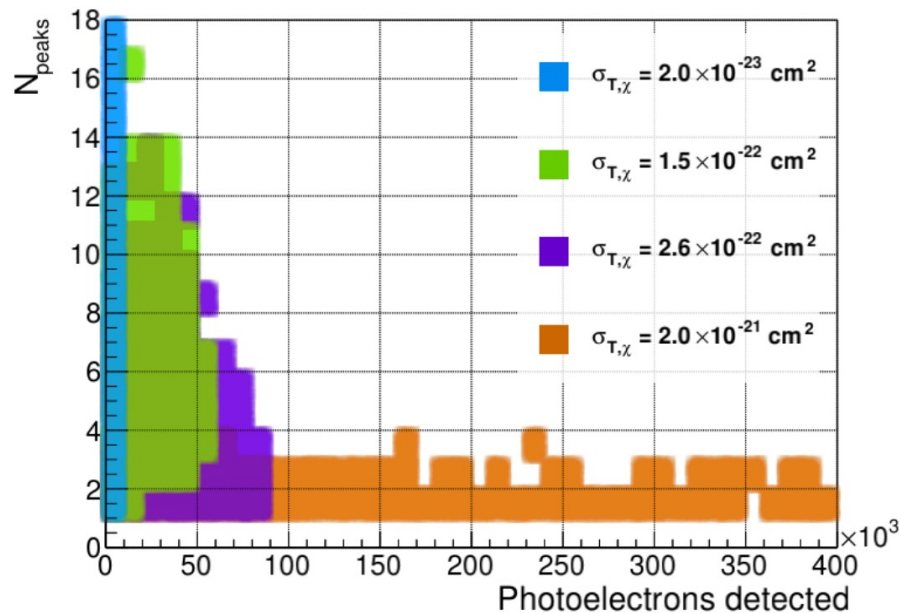
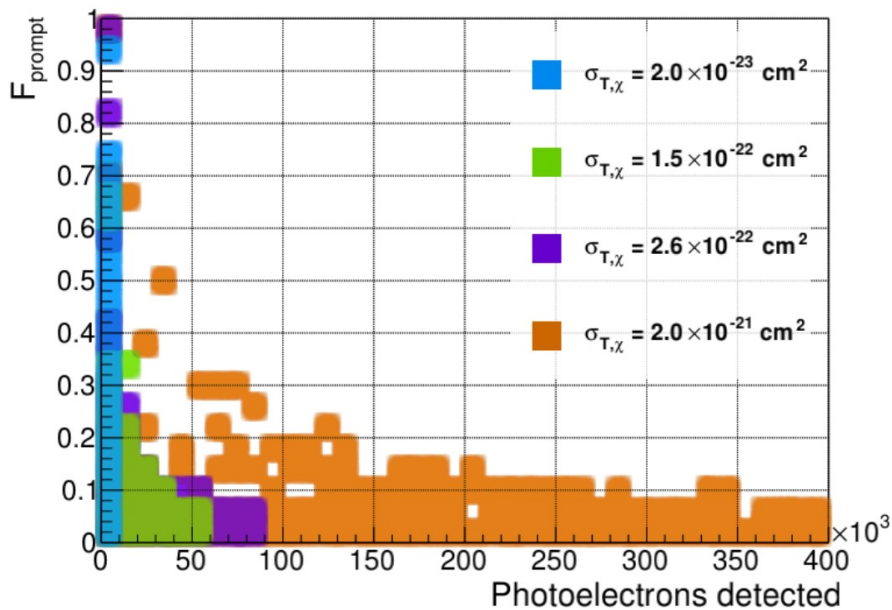


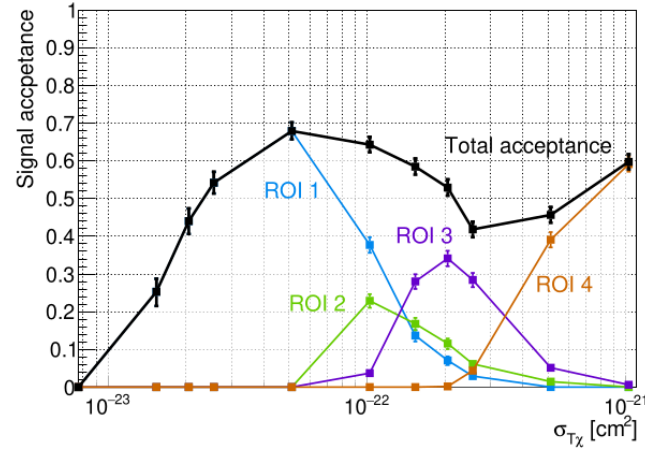
Table 2 Quenching factor of α -particles obtained from the relative measurement using ^{222}Rn , ^{218}Po and ^{214}Po decays within the DEAP-3600 detector. The measured value by Ref. [16] of the QF for α -particles from ^{210}Po decays is also shown.

| Radioactive isotope | Energy of α -particle (MeV) | Ratio of PE peak to ^{222}Rn PE peak (R_i) | Uncertainty on the peak PE ratio (σ_i) | Quenching factor (QF_α) | Uncertainty on QF_α due to PE peak ratios | Absolute uncertainty on QF_α |
|---------------------|------------------------------------|---|---|---|---|--|
| ^{210}Po | 5.305 | - | - | 0.710 [16] | - | 0.028 [16] |
| ^{218}Po | 6.002 | 1.096 | 0.002 | 0.712 | 0.001 | - |
| ^{214}Po | 7.686 | 1.411 | 0.006 | 0.716 | 0.003 | - |

Planck scale mass DM search



Planck scale mass DM search



| ROI | PE range | Energy [MeV _{ee}] | $N_{\text{peaks}}^{\text{min}}$ | $F_{\text{prompt}}^{\text{max}}$ | μ_b | $N_{\text{obs.}}$ |
|-----|-------------------------|-----------------------------|---------------------------------|----------------------------------|-----------------------------|-------------------|
| 1 | 4000–20 000 | 0.5–2.9 | 7 | 0.10 | $(4 \pm 3) \times 10^{-2}$ | 0 |
| 2 | 20 000–30 000 | 2.9–4.4 | 5 | 0.10 | $(6 \pm 1) \times 10^{-4}$ | 0 |
| 3 | 30 000–70 000 | 4.4–10.4 | 4 | 0.10 | $(6 \pm 2) \times 10^{-4}$ | 0 |
| 4 | 70 000– 4×10^8 | 10.4–60 000 | 0 | 0.05 | $(10 \pm 3) \times 10^{-3}$ | 0 |

TABLE I. ROI definitions, background expectations μ_b , and observed event counts $N_{\text{obs.}}$ in the 813 d exposure. A cut rejecting events in a $[-10, 90]$ μs window surrounding each MV trigger is applied to all ROIs; low-level cuts requiring that signals be consistent with bulk LAr scintillation are applied to ROIs 1–3. The upper energy bound on ROI 4 is estimated assuming a constant light yield above 10 MeV_{ee}, the highest energy at which the detector is calibrated.